Theor. Comput. Fluid Dyn. (2016) 30:403–414
DOI 10.1007/s00162-016-0386-9

ORIGINAL ARTICLE

Eugenio Pugliese Carratelli · Giacomo Viccione · Vittorio Bovolin

Free surface flow impact on a vertical wall: a numerical assessment

Received: 12 August 2015 / Accepted: 25 February 2016 / Published online: 18 March 2016

Abstract The sudden impact of a free surface flow upon a solid wall is a common occurrence in many situations in nature and technology. The design of marine structures is probably the most obvious example, but also river and dam hydraulics as well as the necessity of understanding flood and debris flow-induced damage have led to theoretical and experimental work on the mechanism of fluid slamming loads. This is therefore a very old and rich research field, which has not yet reached full maturity, so that semi-empirical methods in design practice are still the rule in many sectors. Up-to-date CFD technology with both Eulerian and Lagrangian approaches is employed to investigate highly non-stationary fluid impact on a solid wall. The development of the pressure wave produced by the impact is examined as it propagates and interacts with the fluid boundaries, as well as the subsequent build-up of high-pressure gradients of high fluid velocities. The geometry and the velocity field of the problem considered are very simple, but the results seem to provide new insight, in particular, into the connection between phenomena with different timescales.

Keywords Fluid impact · Smoothed particle hydrodynamics · Volume of fluid · Fluid–structure interaction · Free surface flows

1 Introduction

The impact of a free surface fluid flow on solid surfaces is of paramount importance in both nature and technology; the literature on the matter is therefore immense, and no attempt can here be made to review it. Some related discussion is reported, for example, in [1–5]. There are many instances in science and technology where this field of study finds applications: the impact of falling objects on a liquid surface [6], liquid sloshing dynamics [7], overtopping flow loads on a dike crest [8,9] and the action of steep sea waves (both breaking and non-breaking) on coastal structures. This latter problem has probably been studied more often than any other and can therefore provide some insight [10–14]. The most recent results in this field consistently show a relatively slow varying loading pattern—often referred to in the literature as "quasi-static"—together with the erratic presence of highly dynamic peak loads, "church steeples". The random nature of such peaks is only natural, since the time behaviour of fluid flow in sea waves is random in itself; they are, however, so erratic in intensity, and of such short duration, that they can only be explained by the interaction of a number of various random and pseudo-random phenomena which are not easy to separate. Theoretical attempts to predict impact pressures have indeed been followed with some success, starting from the pioneering work by Kirkgöz [15], and an extensive discussion of this aspect is reported in [16]. The present work is particularly aimed at clarifying the effects of steep water flow impact, which is part of the general framework of sea wave action.

Communicated by Harindra Joseph Fernando.

E. Pugliese Carratelli · G. Viccione (✉) · V. Bovolin
Department of Civil Engineering, University of Salerno, 84084 Fisciano, Italy
E-mail: gviccion@unisa.it

In the following, a simple and meaningful example, i.e. the impact of an initially steady free surface flow on a vertical wall, will be considered with the object of clarifying some of the various aspects involved. The phenomenon considered here is well understood over a timescale varying from a few tenths to a few seconds ("**long term**", in the following)—among the others see [11]—and it implies the formation of a reflected wave and a basically hydrostatic behaviour. Modern CFD techniques provide a satisfactory explanation of long-term wave action on wall even for more complicated shapes as in [17–19].

On a shorter timescale, i.e. before a reflection wave is formed ("**short term**", in the following), no analytical or numerical solution is available. There are many descriptions of these phenomena, e.g. see [11,20,21], provided incompressible flow solutions for a somewhat similar—but not identical—problem, whereby an idealized and inviscid wave rises against a vertical wall.

Most of the solutions show the formation of a jet-like unsteady flow close to the wall together with the formation of high-pressure gradients; the duration of such pressure peaks is short compared with wave periods, but still of the order of 10^{-1}s.

In many instances, the jet flow flips through the gap in front of the approaching wave forming what is known as a "flip through". Pressure peaks of random or nearly random nature have indeed been often associated with such mechanisms, and various examples of flip-through patterns and of the associate local high pressure have subsequently been found during ad hoc experiments [4,20,22], mostly in the field of sea wave action. Strictly speaking, in this case there is no slamming, in the sense that there is no instantaneous change in velocity at the boundaries

On a yet shorter timescale,"**very short term**", another kind of phenomenon takes place. Soon after wave impact, the hydrodynamic force onto a vertical wall is due to a pressure distribution related to both the fluid compressibility and the celerity of perturbations, i.e. the physical sound speed, numerical terms; a zero normal velocity boundary condition instantaneously appears at the borders of a fluid body, i.e. on some part of the domain border, a sudden change in the conditions takes place, from an assigned boundary pressure p_0 into an assigned normal gradient of velocity $\mathrm{d}v/\mathrm{d}n = 0$. A pressure wave thus develops and propagates with speed $c = \sqrt{\frac{\partial p}{\partial \rho}}$, which would behave very much like the classical water hammer Joukowsky effect [23,24], except for the different boundary conditions on the upper surface. This aspect, which in the following we shall define as "slamming", is highly significant in connection with very short-term pressure evolution and has been—among others—treated in [25,26]. In particular, Korobkin [25] provided an analytical solution related to a similar problem in which, however, the fluid mass was entirely bounded, thus preventing any macroscopic movement of the fluid and any subsequent hydrodynamic development of the free surface.

A number of papers by Peregrine and co-workers also deal with such a very short-term impact, e.g. [27]. The pressure wave is considered within a very short time window, yielding a so-called pressure—impulse model. However, their solutions does not provide details of the pressure field.

A timescale for such initial phase can be given by the ratio between a typical dimension such as the initial water height h_0 and the celerity c, i.e. h_0/c. Assuming h_0 to be of the order of one metre and $c = 1410$ m/s, the timescales turns out to be of about 10^{-3}s or less, thus justifying the notion of "very short term" given above.

It is thus clear that even for a simple geometry such as the one considered here, there is as yet no general picture of the phenomena encompassing three different timescales: the transition between the available results, and even their applicability, is therefore confused.

In the present paper, in order to clarify the development of the pressure and flow fields from the "very short term" through the "short term" to the "long term", a numerical investigation is carried out by tackling compressible Navier Stokes equations for the test case described above. Due to the physical and computational difficulty of the problem, two different approaches—Eulerian and Lagrangian—are followed in parallel in order to cross-check some of the more delicate aspects.

The situation considered here is an open channel flow, with an initially steady velocity "v_0" and an initially uniform height "h_0", which suddenly impacts with a vertical wall; while abstract in its physical formulation, such a set up can be considered to represent with some approximation various real-life situations, such as the collision of broken waves against a breakwater. It is worth mentioning at this regard that a broad range of open channel flows, either steady or unsteady, can be simulated with the smoothed particle hydrodynamics (SPH) technique thanks to an advanced procedure proposed in [28,29], able to properly enforce boundary flow conditions.

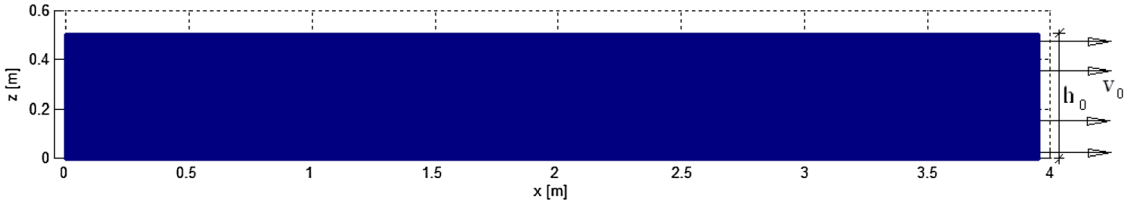

Fig. 1 Initial flow conditions: liquid height $h_0 = 0,50$ m, liquid velocity $v_0 = 10$ m/s

2 Methodology

In order to clarify the development of the pressure and flow fields from the "**very short term**" through the "**long term**", a numerical investigation is carried out by numerically integrating Navier Stokes equations for the test case described in the following.

An open channel flow with an initial velocity $v_0 = 10$ m/s and water height $h_0 = 0.50$m is assumed to impact suddenly against a vertical wall (Fig. 1). For computational purposes, a 4.00-m-long volume of fluid was assumed. The highly non-stationary conditions are so extreme that the authors have maintained that in order to gain full confidence in the results, two completely different approaches were necessary: Eulerian, based on Flow3D®, a commercial package, and Lagrangian, by making use of the weakly compressible smoothed particle hydrodynamics (WCSPH) technique, an SPH solver developed by the authors.

2.1 The WCSPH model

The Lagrangian code developed by the authors, based on the well-known WCSPH (weakly compressible smoothed particle hydrodynamics) technique—see [30–33] for recent comprehensive reviews and related applications—has been employed for the very short-term impact analysis. Recently, SPH has been considered as valuable method for solving real-life engineering problems in maritime context as in [34–40]. In [41], a full SPH-based framework for solving problems involving large fluid motion and large structural deformations and failure was proposed. Altomare et al. [42] carried advanced investigations of wave interaction with Armour block sea breakwater. Three-dimensional dam break propagation and impact of liquids have been investigated by Ferrari et al. [43] by means of a parallel SPH algorithm. Shao et al. [44] proposed the method coupled with Reynolds-averaged Navier–Stokes (RANS) turbulence model for simulating viscous incompressible liquid sloshing dynamics, including corrections on the density and kernel gradient representation.

The procedure here adopted has been widely applied and validated in a number of situations, see, for instance, [45–49].

Briefly summarizing, Navier–Stokes equations

$$-\frac{1}{\rho}\frac{\mathrm{D}\rho}{\mathrm{D}t} = \nabla \cdot \underline{v} \tag{1a}$$

$$\rho\frac{\mathrm{D}\underline{v}}{\mathrm{D}t} = -\nabla p + \mu\nabla^2\underline{v} + \underline{f} \tag{1b}$$

are discretized by making use of a finite collection of pseudo-particles, as in [45],

$$\frac{\mathrm{D}\log(v_i)}{\mathrm{D}t} = \sum_{j=1}^{N_i}\left(\underline{v}_i - \underline{v}_j\right)\cdot\nabla_i W_{ij}\cdot\mathrm{d}\Omega_j + \xi h c_0\sum_{j=1}^{N_i}\psi_{ij}\cdot\nabla_i W_{ij}\cdot\mathrm{d}\Omega_j \tag{2a}$$

$$\frac{\mathrm{D}\underline{v}_i}{\mathrm{D}t} = -\sum_{j=1}^{N_i}\left(\frac{p_i}{\rho_i} + \frac{p_j}{\rho_j} + 19.6\nu\left(\frac{\underline{v}_{ij}\cdot\underline{r}_{ij}}{r_{ab}^2 + \varepsilon\overline{h}_{ij}^2}\right)\right)\nabla_i W_{ij}\mathrm{d}\Omega_j + \underline{f}_i \tag{2b}$$

with the following meaning of the symbols: i denotes the generic moving particle, j refers to one of its N_i neighbours, and v_i is the specific volume $1/\rho_i$, whose definition is recalled in the following:

$$\frac{\mathrm{D}\log(v_i)}{\mathrm{D}t} = -\frac{1}{\rho_i}\frac{\mathrm{D}\rho_i}{\mathrm{D}t} = \nabla\cdot\underline{v}_i \tag{3}$$

ρ is the density, p is the pressure, $\underline{v}$ is the velocity vector, $\underline{f}$ is the external force, W is the so-called kernel or weighting function defined over a compact support of radius $r = 2h$, being $h = 1.3d_0$ the smoothing length proportional to the initial interparticle distance d_0, $\nu = 10^{-6}\ \mathrm{m^2/s}$ is the kinematic viscosity of water at 20 °C (no temperature dependency was taken into account), and c_0 is the speed of sound in the case of no compression, that is with the reference density of the fluid $\rho = \rho_0 = 1000\,\mathrm{kg/m^3}$. In this work, we inquire into the propagation of pressure wave, so we try to mimic the real celerity with the artificial SPH "speed of sound".

Equations (2), constrained with (3) and coupled with the Tait equation of state [50]

$$p_i = \frac{c_0^2\rho_0}{\gamma}\left[\left(\frac{\rho_i}{\rho_0}\right)^{\gamma} - 1\right] \tag{4}$$

being $\gamma = 7$, is then solved in time with the second-order predictor–corrector step scheme, next specified

$$\text{predictor step: } \begin{cases} M_i^{n+1,*} = M_i^n + \Delta t N_i^n \\ \underline{v}_i^{n+1,*} = \underline{v}_i^n + \Delta t\,\underline{a}_i^n \\ \underline{x}_i^{n+1,*} = \underline{x}_i^n + \Delta t\,\underline{v}_i^n + \frac{\Delta t^2}{2}\underline{a}_i^n \end{cases} \qquad \text{corrector step: } \begin{cases} M_i^{n+1} = M_i^n + \Delta t\frac{N_i^n + N_i^{n+1,*}}{2} \\ \underline{v}_i^{n+1} = \underline{v}_i^n + \Delta t\frac{\underline{a}_i^n + \underline{a}_i^{n+1,*}}{2} \\ \underline{x}_i^{n+1} = \underline{x}_i^{n+1,*} \end{cases} \tag{5}$$

where

$$M_i = \log(v_i), \quad N_i = \left[\frac{\mathrm{d}}{M}\mathrm{d}t\right]_i, \quad \underline{a}_i = \left[\frac{\mathrm{d}\underline{v}}{\mathrm{d}t}\right]_i, \underline{v}_i = \left[\frac{\mathrm{d}\underline{x}}{\mathrm{d}t}\right]_i \tag{6}$$

The integration time Δt appearing in Eqs. (5) is constrained to the Courant–Friedrichs–Levy (CFL) stability condition, for which

$$\Delta t = \mathrm{CFL}\min_{i=1,\ldots,N_p}\frac{h}{c_0(1+\xi/4) + |\underline{v}_i| + \zeta_i} \tag{7}$$

where

$$\zeta_i = h\max_{j=1,\ldots,N_{p,i}}\frac{\left|\left(\underline{v}_i - \underline{v}_j\right)\cdot\left(\underline{x}_i - \underline{x}_j\right)\right|}{\left|\underline{x}_i - \underline{x}_j\right|^2} \tag{8}$$

being N_p the total number of particles, either of fluid or solid type, N_{pj} the total number of neighbouring particles of the pointed particle i. The scheme is stable for the adopted Courant number CFL = 0.25. The classical cubic spline approach is followed, and the Newtonian viscous stress term is modelled by implementing the linear part of the artificial viscosity of Monaghan and Gingold [51] as proposed by Cleary [52]. In particular, Cleary determined the coefficient 19.6 by carrying out a campaign of numerical experiments in two dimensions. His further investigations suggested a coefficient slightly different—20—for three-dimensional problems. A recent discussion of the effects of the artificial viscosity in SPH computations modelling regular breaking waves is reported in [53]. The additional terms ξ and ψ_{ij}, appearing inside the diffusion term, are implemented as suggested in [54]. They are meant to filter out high-frequency spurious pressure oscillations. The applied correction is consistent in terms of mass conservation for the short-time simulations being carried out. Besides the numerical effects, the diffusive coefficient ξ, which in this work was taken to be 0.1, has also a physical meaning as "expansion" or "bulk" viscosity, see, for instance, [50]. This technique yields good results in terms of pressure distributions and overcomes limits encountered in [55].

Particle methods have been used to cope with similar problems as such those mentioned before, for instance by [56], in which the SPH technique is used for modelling the impact of an elastic cylinder against a flat fluid surface, a problem which in the very short terms bears a close resemblance with fluid slamming. Since the

application is rather new, however, some problems had to be dealt with, in order to assess its applicability to the problem at hand.

A first difficulty might arise in the boundary conditions, a vital aspect in slamming problems. The fixed boundaries are represented by a collection of non-moving particles placed around the simulation domain simulation domain. When a fluid particles i is approaching onto a boundary particle j, a repulsive force $\underline{f}_{ij}$ resulting from an increase in interstitial pressure term prevents particles compenetration; this is standard practice in SPH work, but it is often modified by providing an extra short-range repulsive force which—by analogy with molecular interaction—is called "Lennard–Jones" (LJ) [57]:

$$\underline{f}_{ij} = \begin{cases} D\left[\left(\frac{\mathrm{d}_0}{|\underline{x}_i - \underline{x}_j|}\right)^{P_1} - \left(\frac{\mathrm{d}_0}{|\underline{x}_i - \underline{x}_j|}\right)^{P_2}\right] \frac{\underline{x}_i - \underline{x}_j}{|\underline{x}_i - \underline{x}_j|} \frac{\mathrm{d}_0}{|\underline{x}_i - \underline{x}_j|} > 1 \\ 0 \frac{\mathrm{d}_0}{|\underline{x}_i - \underline{x}_j|} \leq 1 \end{cases} \tag{9}$$

According to [58], we set $D = 5\,\mathrm{g\,h_0}$, $p_1 = 12$ and $p_2 = 6$. The authors have carried out extensive SPH tests, with and without LJ forces, and have found out [59] that the dynamics are not remarkably affected by the presence of such an additional term.

The proposed procedure can thus provide reliable results in this kind of problems, if at the price of a heavy computational effort. The domain is divided into 79.000 pseudo-particles, with an initial interparticle distance $d_0 = 0.005$m.

2.2 The Flow3D model

Flow3D solver [60] is a CFD software system originally developed at Los Alamos Laboratory. It is based on a finite volume formulation of the Navier Stokes equations in a Eulerian framework. Free surfaces and interfaces are solved with the volume of fraction (VOF) method and the fractional area/volume obstacle representation. Velocity and pressure fields are coupled by using the time-advanced velocities in the continuity equations and time-advanced pressures in the momentum equations. The model has been widely validated over the years particularly in connection with wave impact, see, for instance, [61,62].

The integration is performed in time with a two-step momentum predictor-continuity corrector procedure. The corrector step makes use of a weakly compressible approach, whereby in the continuity equation, a variable density mass flow is considered and the compressibility is simulated through a linear law—the acoustic approximation—which links the density variation to the pressure increase $c^2 = \partial p/\partial \rho$. No additional dissipation term is included in the momentum equation, so this approach is valid for low Mach numbers and is consistent with the acoustical approximation reported in much of the current literature [63]. All the tests shown in the following have bee carried out by assuming a fluid with density $\rho_0 = 1000\,\mathrm{kg/m^3}$ and a compressibility parameter $k = 1/\rho_0 c_0^2$ taken to provide the same sound speeds $c_0 = 1400$ m/s and $c_0 = 700$ m/s, as in the SPH model. The chosen values, representing realistic liquids, satisfy the acoustic condition $|\delta\rho/\rho| < 0.1$ as the Mach number is of order 10^{-2} or less.

The same geometric and cinematic conditions are here assumed as in Paragraph 2.1. The obvious difference relies on the discretization: the computation domain is split into square 0.01-m-wide grid elements. After the appropriate convergence testing, an optimal grid (cell spacing $\Delta x = 0.01$m, $\Delta y = 0.01$m, total number of cells $N_{\mathrm{cell}} = 2 \times 10^4$) was selected. The integration time step, bound by the Courant constraints $\Delta t < \mathrm{d}x/c_0$, allows a reasonable computation time throughout the very short and the short to the long timescale.

3 Results and discussion

3.1 Comparative results on very short term

The following Figs. 2 and 3 show results in terms of pressure contour, employing SPH (left side) and Flow3D (right side), at various time instants. Reference sound speeds are $c_0 = 1400$ m/s and $c_0 = 700$ m/s, respectively. Computing time (CT) is expressed with respect to the beginning of the simulation, whereas the simulation time (ST) is measured from the impact instant. A single colour scale for pressure is assumed, in order to make the comparison easier. Pressure peak (p_p) is specified as well.

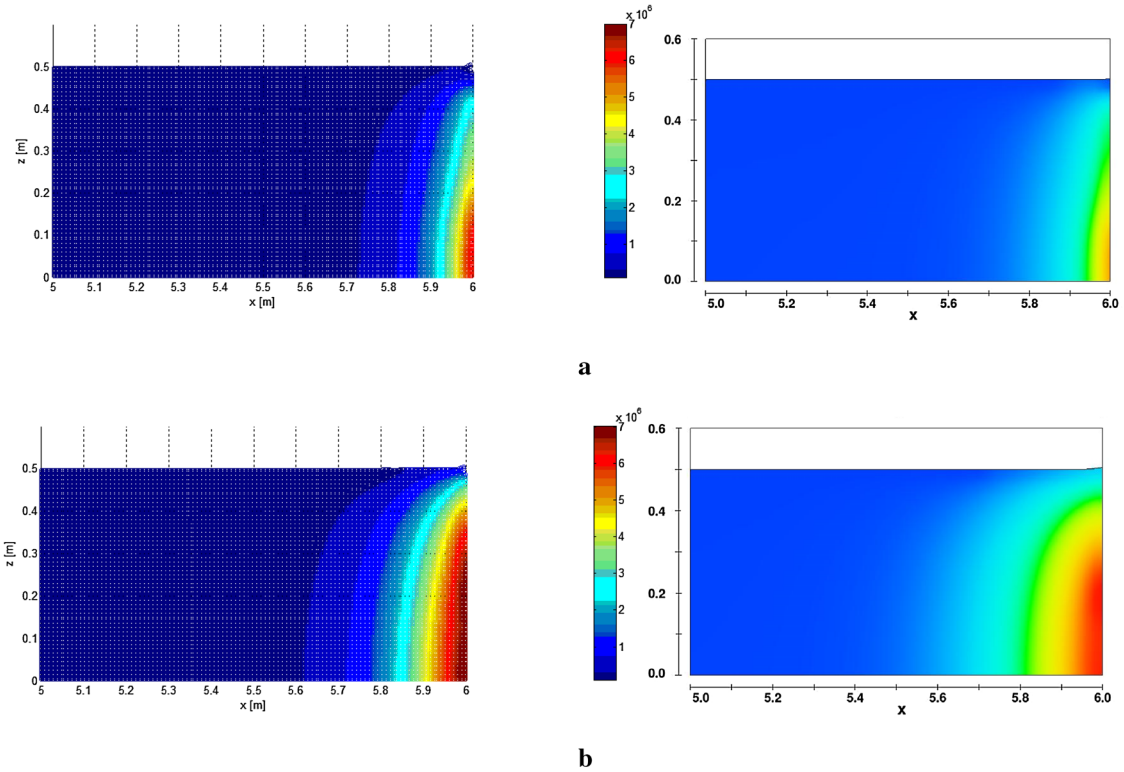

Fig. 2 Very short-term analysis. Pressure field comparison between SPH and Flow3D with $c_0 = 700$ m/s. **a** *Left* (SPH), CT $= 6.5 \times 10^3$ s, $p_p = 5.88 \times 10^6$ Pa. *Right* (Flow3D), CT $= 1.5 \times 10^3$ s, $p_p = 4.75 \times 10^6$ Pa. ST $= 3 \times 10^{-4}$ s. **b** *Left* (SPH), CT $= 1.1 \times 10^4$ s, $p_p = 6.94 \times 10^6$ Pa. *Right* (Flow3D), CT $= 2.5 \times 10^3$ s, $p_p = 6.18 \times 10^6$ Pa. ST $= 5 \times 10^{-4}$ s

Both methods, SPH and Eulerian, reproduce a similar build-up and evolution of a high-pressure field, as it would be expected according to the Joukowsky formula $\Delta p = \rho_0 c_0 \Delta v$, with $\Delta v = v_0 = 10$ m/s. A stiffer response is generally given by the SPH model. Anyway, pressure values at a specific time instant are of the same order of magnitude.

A pressure front is generated at the impact along the vertical wall and travels with its own celerity; if the upper surface were rigid, it would simply travel backwards as in an ordinary water hammer effect. Since, however, the surface is free, a pressure wave of the opposite sign develops and moves downwards, justifying the peculiar pressure wave shape. It is worth noticing that no significant jet has yet formed along the wall.

In the following, a comparison between maximum pressure peaks (mpp), obtained with SPH and Flow3D, and the Joukowsky pressure p_J is provided (Table 1).

3.2 Comparative results on short term

After about 5×10^{-4} s, most of the Joukowsky pressure wave generated by the slamming effect has disappeared; following that, a new pressure spot starts building up again at a slower rate (Figs. 4, 5).

This increase, though much lower, is quite distinct and is possibly due an entirely new mechanism, which involves the formation of a vertical jet and a localized area of high pressure at approximately the still water level.

Despite some differences between the two solutions, it is easy to see that this area of increased pressure is consistently located where particle trajectories make a tighter bend and undergo a strong vertical acceleration; compressibility plays little or no role in this phenomenon, which is conceptually similar to the analytical inviscid and incompressible flow solution reported in [11].

It is thus evident that there are two different mechanism that produce high-pressure transients: the first—which we defined as "very short term "—generates a very high peak whose duration is of the order h_0/c and is basically the phenomenon which was studied by [26,27]; the second, which takes place in the "short term",

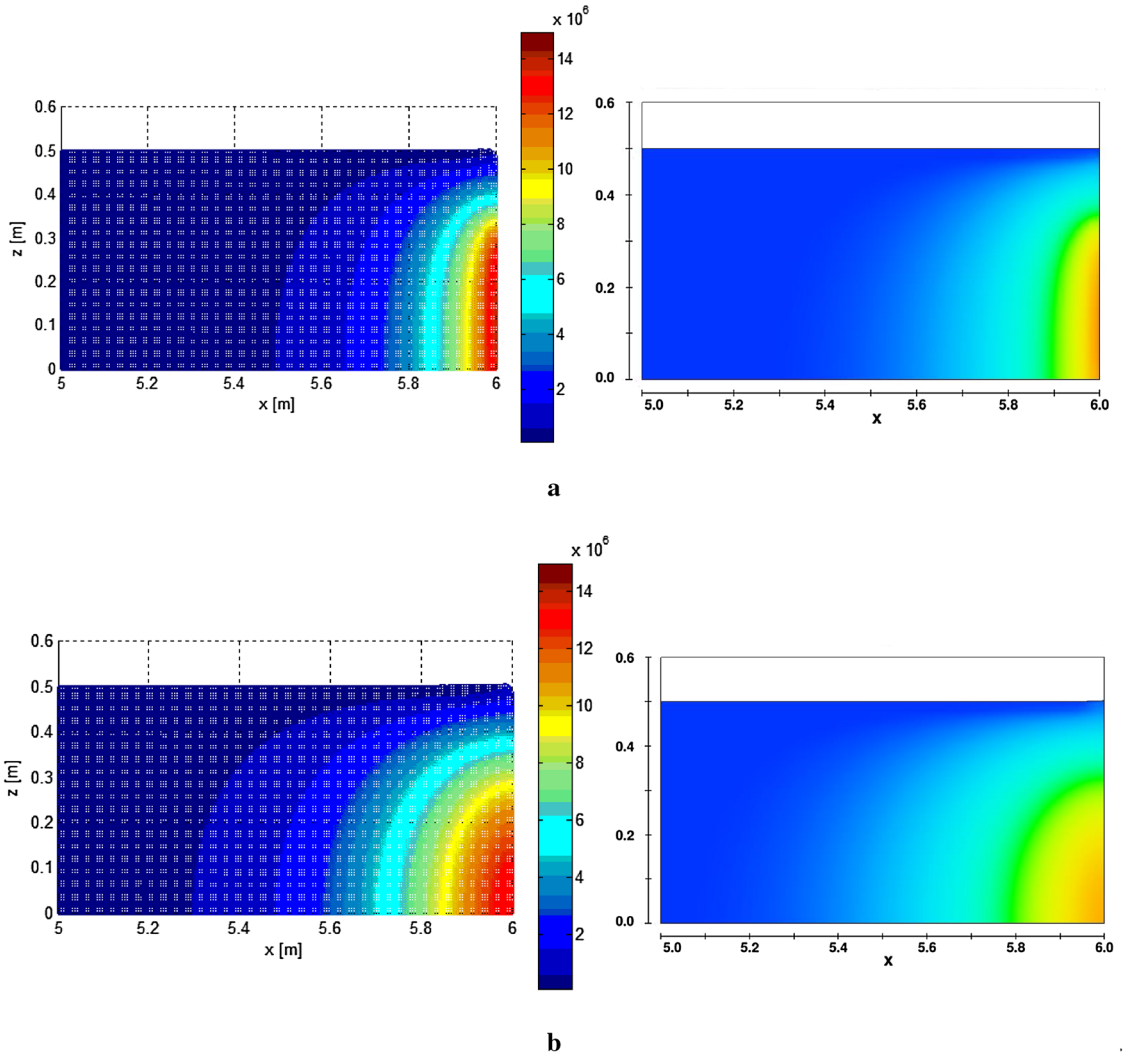

Fig. 3 Very short-term analysis. Pressure contour comparison between SPH and Flow3D with $c_0 = 1400$ m/s. **a** *Left* (SPH), CT $= 1.4 \times 10^4$ s, $p_\mathrm{p} = 1.38 \times 10^7$ Pa. *Right* (Flow3D), CT $= 2.9 \times 10^3$ s, $p_p = 1.13 \times 10^7$ Pa. ST $= 3 \times 10^{-4}$ s. **b** *Left* (SPH), CT $= 2.3 \times 10^4$ s, $p_\mathrm{p} = 1.31 \times 10^7$ Pa. *Right* (Flow3D), CT $= 4.7 \times 10^3$ s, $p_\mathrm{p} = 1.04 \times 10^7$ Pa. ST $= 5 \times 10^{-4}$ s

Table 1 Maximum pressure peaks obtained numerically as function of celerity C_0 compared with the Joukowsky pressure

c_0 (m/s)	mpp (SPH) (MPa)	mpp (Flow3D) (MPa)	p_J (MPa)
700	6.9	6.2	7
1400	13.8	11.3	14

is much smaller in intensity but longer in duration: it is the equivalent, in a simpler geometry, of Peregrine's wave impact as in [11].

In many real-life cases, the "shot-term" and the "very short-term" effects are actually superimposed and this might explain some problems in the interpretation of real-life impact effects.

3.3 Long term with Flow3D

In the following, the "long-term"—i.e. a few tenth of seconds—time evolution of the impact process is shown as obtained with Flow3D. The WCSPH model is not used here, because the adopted scheme yields a substantial loss of the mechanical energy over long runs.

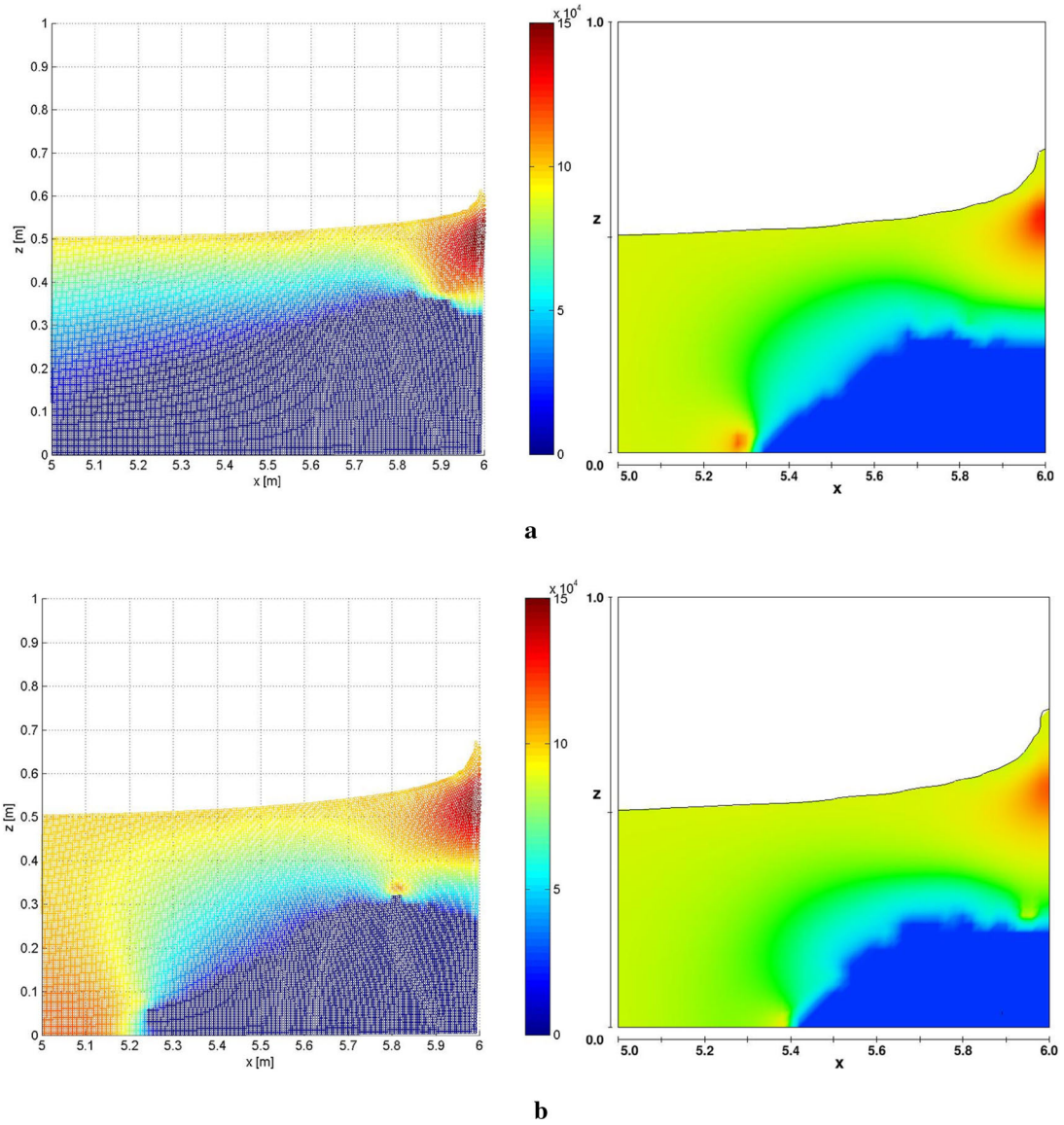

Fig. 4 Short-term analysis. Pressure contour comparison between SPH and Flow3D with $c_0 = 700$ m/s. **a** *Left* (SPH), CT $= 2.3 \times 10^4$ s, $p_p = 1.48 \times 10^5$ Pa. *Right* (Flow3D), CT $= 4.9 \times 10^3$ s, $p_p = 1.42 \times 10^5$ Pa. ST $= 0.009$ s. **b** *Left* (SPH), CT $= 2.4 \times 10^4$ s, $p_p = 1.45 \times 10^5$ Pa. *Right* (Flow3D), CT $= 5.0 \times 10^3$ s, $p_p = 1.37 \times 10^5$ Pa. ST $= 0.010$ s

Over such a timescale, as it is well known, the unsteady flow structure can take two basic patterns, depending upon the ratio between inertia and gravity: if inertia prevails upon gravity, the flow deviates vertically; otherwise, the whole flow decelerates and a reflected surface wave is generated. The relevant indicator is Froude number

$$F_r = \frac{V_0}{\sqrt{g \cdot h_0}} \tag{10}$$

Numerical simulation of the long-term dynamics is much less critical and can be carried under incompressible fluid hypothesis. In any case, pressure gradients are nearly hydrostatic as in [15], see 'Secondary impact pressure' section. Figure 6 shows the typical behaviour for Fr $= 2.86$ and Fr $= 0.1$, respectively

The behaviour at high Fr number is particularly interesting, as it implies the fall back of the jet flow over on the fluid body and the formation of a macroscopic fluid flow; the phenomenon, however, has been thoroughly investigated [11,64–66], and it is beyond the scope of this paper.

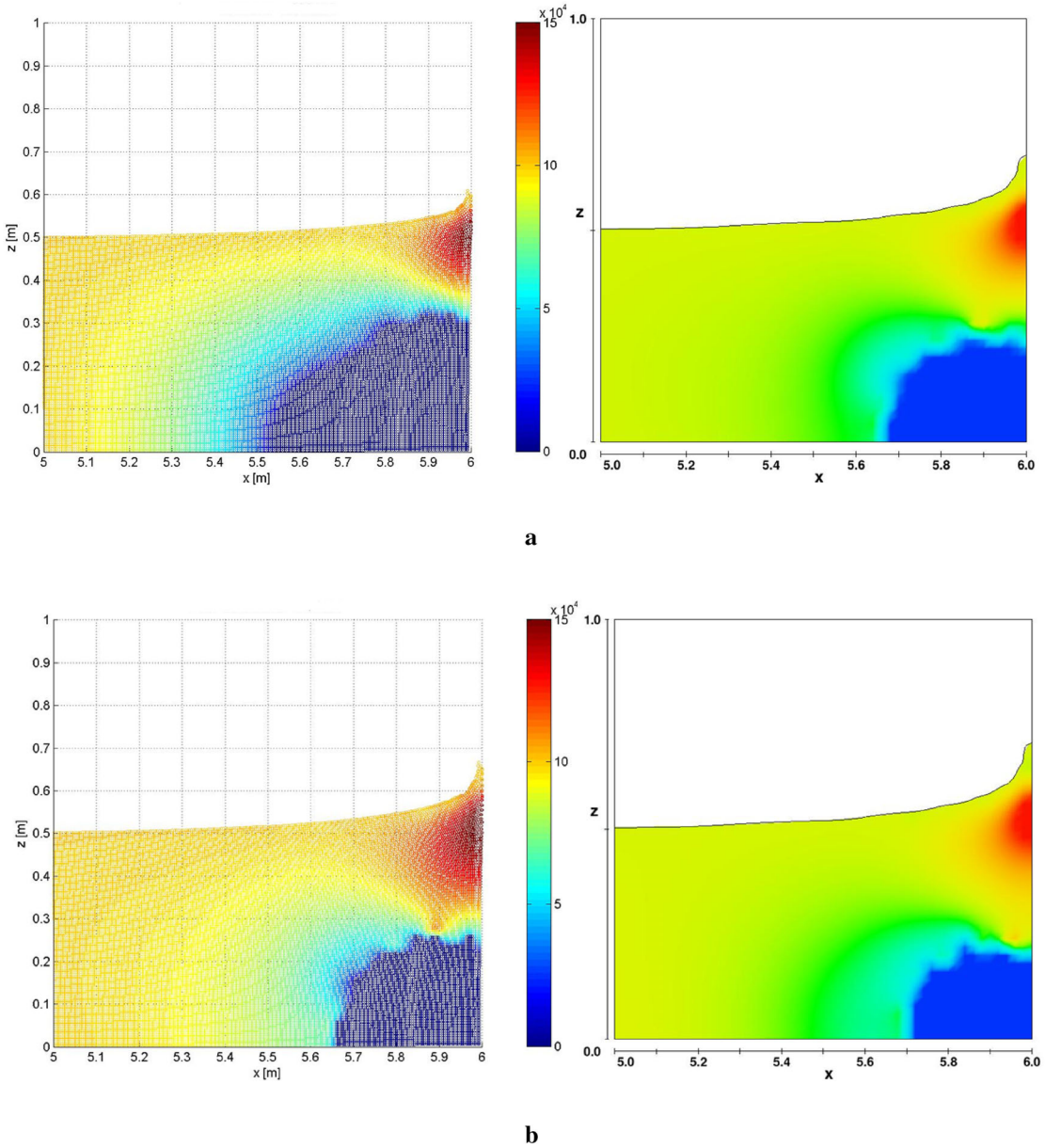

Fig. 5 Short-term analysis. Pressure contour comparison between SPH and Flow3D with $c_0 = 1400$ m/s. **a** *Left* (SPH), CT $= 4.7 \times 10^4$ s, $p_p = 1.50 \times 10^5$ Pa. *Right* (Flow3D), CT $= 9.9 \times 10^3$ s, $p_p = 1.42 \times 10^5$ Pa. ST $= 0.009$ s. **b** *Left* (SPH), CT $= 4.7 \times 10^4$ s, $p_p = 1.55 \times 10^5$ Pa. *Right* (Flow3D), CT $= 9.9 \times 10^3$ s, $p_p = 1.46 \times 10^5$ Pa. ST $= 0.010$ s

4 Conclusions

The numerical experiments carried out on the sudden fluid impact of an open surface fluid flow on a vertical wall have highlighted the presence of three well-distinct classes of phenomena, each with its own different time span. The first effect yields a pressure wave with the peak in accordance with the Joukowsky equation, though modified and attenuated by the presence of the free surface; the second one is a non-compressible flow mechanism and involves the formation of a jet on the surface in connection with a localized high-pressure area; the third one correspond to a nearly hydrostatic pressure distribution and is linked to the propagation of a reflected surface wave.

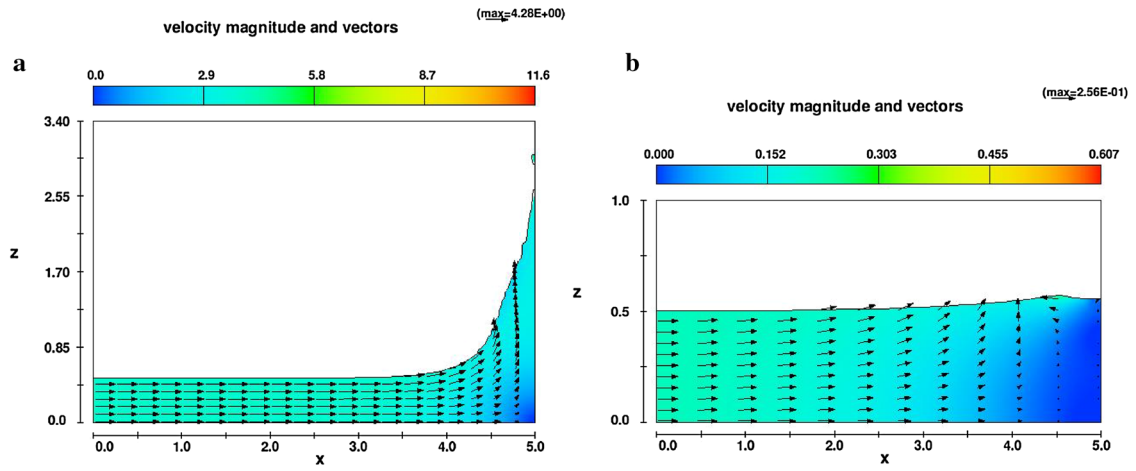

Fig. 6 Long-term flow patterns. **a** Jet-like flow, ST = 2.0 s. **b** Reflected wave ST = 2.0 s

While each of the three mechanisms, with their different timescales, has been investigated before, the numerical approach illustrated in the paper encompasses all of the three regimes in a single framework and should help to clarify and locate in a proper context some of the real-life experimental results.

For instance, in the domain of sea wave impact, it is generally acknowledged that forces and pressure upon the wall are associated with the formation of a reflected wave, giving rise to a "long-term" (in our terminology) effect; in addition, highly variable random forces and pressures often appear (church steeples), and this effected is often linked to the formation of a flip-through and to the related narrow curvature trajectories, as originally described in [64] and confirmed experimentally by others, see, for example, [65]. This is close to what we have described above as "short-term" effects; the results presented here, however, suggest that a different and "very short" slamming effect has also to be taken into account, with a very high pressure increase and a timescale of the order of h_0/c, where h_0 is a typical length scale for the impact area, i.e. a few thousandth of second for real structures, and tenths of thousandth for laboratory experiments. It is thus most likely that such very high-pressure bursts are not normally revealed by ordinary tank tests while still potentially carrying relevant consequences. Where careful tests with high-frequency data sampling have been carried out, this view seems to be confirmed, e.g. by [16], who give detailed results of impact peak loads which are congruent with the data produced here.

Acknowledgments This research has been supported through the FARB project "Developing of numerical models for the simulation of wave propagation and impact processes", scientific responsible: Giacomo Viccione, code number ORSA139472. All the computations were carried out on the Opteron quad processor machine and other computers, as well as on software systems owned and maintained @ C.U.GR.I. (Centre for Research on Major Hazards), a partnership between the University of Salerno and "Federico II" in Naples.

References

1. Belytschko, T.: Fluid–structure interaction. Comput. Struct. **12**(4), 459–469 (1980)
2. Guruswamy, P.: A review of numerical fluids/structures interface methods for computations using high-fidelity equations. Comput. Struct. **80**(1), 31–41 (2002)
3. Frémond, M., Gormaz, R., San Martìn, J.A.: Collision of a solid with an incompressible fluid. Theor. Comput. Fluid Dyn. **16**, 405–420 (2003)
4. Peseux, B., Gornet, L., Donguy, B.: Hydrodynamic impact: numerical and experimental investigations. J. Fluid. Struct. **21**, 277–303 (2005)
5. Korobkin, A.A., Gueret, R., Malenica, S.: Hydroelastic coupling of beam finite element model with Wagner theory of water impact. J. Fluid. Struct. **22**, 493–504 (2006)
6. Khabakhpasheva, T.I., Korobkin, A.A.: Elastic wedge impact onto a liquid surface: Wagner's solution and approximate models. J. Fluid Struct. **36**, 32–49 (2013)
7. Bulian, G., Botia-Vera, E., Souto-Iglesias, A.: Experimental sloshing pressure impacts in ensemble domain: transient and stationary statistical characteristics. Phys. Fluids **26**(3), 30 (2014)
8. Chen, X., Hofland, B., Altomare, C., Suzuki, T., Uijttewaal, W.: Forces on a vertical wall on a dike crest due to overtopping flow. Coast. Eng. **95**, 94–104 (2015)

9. Chen, X., Hassan, W., Uijttewaal, W., Verwaest, T., Verhagen, H.J., Suzuki, T., Jonkman, S.N.: Hydrodynamic Load on the Building caused by Overtopping Waves. Coast. Eng. Proc. **33**, 11 (2012)
10. Dentale, F., Donnarumma, G., Pugliese Carratelli, E.: Simulation of flow within armour blocks in a breakwater. J. Coast. Res. **30**(3), 528–536 (2014)
11. Peregrine, D.H.: Water wave impact on walls. Annu. Rev. Fluid Mech. **35**, 23–43 (2003)
12. Cuomo, G., Piscopia, R., Allsop, W.: Evaluation of wave impact loads on caisson breakwaters based on joint probability of impact maxima and rise times. Coast. Eng. **58**(1), 9–27 (2011)
13. Faltinsen, O.M., Landrini, M., Greco, M.: Slamming in marine applications. J. Eng. Math. **48**(3–4), 187–217 (2004)
14. Peregrine, D.H., Bredmose, H., Bullock, G., Obhrai, C., Müller, G., Wolters, G.: Violent water wave impact on a wall. In: Proceedings of 14th Aha Huliko Winter Workshop, Honolulu, Hawaii (2005)
15. Kirkgöz, M.S.: Breaking wave impact on vertical and sloping coastal structures. Ocean Eng. **22**, 35–48 (1995)
16. Cuomo, G., Allsop, W., Bruce, T., Pearson, J.: Breaking wave loads at vertical seawalls and breakwaters. Coast. Eng. **57**(4), 424–439 (2010)
17. Al-Banaa, K., Liu, P.L.F.: Numerical study on the hydraulic performance of submerged porous breakwater under solitary wave attack. J. Coast. Res. **50**, 201–205 (2007)
18. Dentale, F., Donnarumma, G., Pugliese Carratelli, E.: Numerical wave interaction with tetrapods breakwater. Int. J. Nav. Arch. Ocean **6**, 13 (2014)
19. Meringolo, D.D., Aristodemo, F., Veltri, P.: SPH numerical modeling of wave–perforated breakwater interaction. Coast. Eng. **101**, 48–68 (2015)
20. Bullock, G., Obhrai, C,. Müller, G., Wolters, G., Peregrine, D.H., Bredmose H.: Field and laboratory measurements of wave impacts. In: Proceedings of the 3rd Coastal Structures Conference, Portland, Oregon (2003)
21. Korobkin, A.: Asymptotic theory of liquid–solid impact. Philos. Trans. R. Soc. A. **35**, 507–522 (1997)
22. Lugni, C., Brocchini, M., Faltinsen, O.M.: Wave impact loads: the role of the flip-through. Phys. Fluids **18**(12), 101–122 (2006)
23. Joukowsky, N.: Über den hydraulischen Stoss in Wasserleitungsröhren." ("On the hydraulic hammer in water supply pipes."). Mémoires de l'Académie Impériale des Sciences de St.-Pétersbourg (1900)
24. Simin, O.: Water hammer. In: Proceedings of 24th Annual Convention of the American Water Works Association, pp. 341–424. St. Louis, USA (1904)
25. Korobkin, A.: Global characteristics of jet impact. J. Fluid Mech. **307**, 63–84 (1996)
26. Korobkin, A., Khabakhpasheva, T.I.: Plane problem of asymmetrical wave impact on an elastic plate. J. Appl. Mech. Tech. Phys. **39**(5), 782–791 (1998)
27. Wood, D.J., Peregrine, D.H., Bruce, T.: Study of wave impact against a wall with pressure-impulse theory. Part 1: trapped air. J. Waterw. Port C-ASCE **126**, 182–190 (2000)
28. Federico, I., Marrone, S., Colagrossi, A., Aristodemo, F., Antuono, M.: Simulating 2D open-channel flows through an SPH model. Eur. J. Mech. B-Fluid **34**, 35–46 (2012)
29. Aristodemo, F., Marrone, S., Federico, I.: SPH modeling of plane jets into water bodies through an inflow/outflow algorithm. Ocean Eng. **105**, 160–175 (2015)
30. Monaghan, J.J.: Smoothed Particle Hydrodynamics. Rep. Progr. Phys. **68**(8), 1703–1759 (2005)
31. Gómez-Gesteira, M., Rogers, B.D., Dalrymple, R.A., Crespo, A.J.C.: State-of-the-art of classical SPH for free-surface flows. J. Hydraul. Res. **48**(Extra Issue), 6–27 (2010)
32. Viccione, G., Bovolin, V., Pugliese Carratelli, E.: Simulating flows with SPH: recent developments and applications. In: Intech hydrodynamics—optimizing methods and tools, pp. 69–84 (2011)
33. Violeau, D.: Fluid Mechanics and the SPH Method: Theory and Applications. Oxford University Press, Oxford (2012)
34. Altomare, C., Crespo, A.J.C., Domínguez, J.M., Gómez-Gesteira, M., Suzuki, T., Verwaest, T.: Applicability of smoothed particle hydrodynamics for estimation of sea wave impact on coastal structures. Coast. Eng. **95**, 94–104 (2015)
35. Amicarelli, A., Albano, R., Mirauda, D., Agate, G., Sole, A., Guandalini, R.: A Smoothed Particle Hydrodynamics model for 3D solid body transport in free surface flows. Comput. Fluids **116**, 205–228 (2015)
36. Aristodemo, F., Meringolo, D.D., Groenenboom, P., Lo Schiavo, A., Veltri, P., Veltri, M.: Assessment of dynamic pressures at vertical and perforated breakwaters through diffusive SPH schemes. Math. Probl. Eng., 2015, 305028 (2015). doi:10.1155/2015/305028
37. Barreiro, A., Crespo, A.J.C., Domínguez, J.M., Gómez-Gesteira, M.: Smoothed particle hydrodynamics for coastal engineering problems. Comput. Struct. **120**, 96–106 (2013)
38. Stansby, P.K.: Coastal hydrodynamics—present and future. J. Hydraul. Res. **51**(4), 341–350 (2013)
39. Groenenboom, P.H.L., Cartwright, B.K.: Hydrodynamics and fluid–structure interaction by coupled SPH-FE method. J. Hydraul. Res. **48**(Extra Issue), 61–73 (2010)
40. Dalrymple, R. A., Knio, O. M.: SPH modelling of water waves. In: Proceedings of Coastal Dynamics ASCE, pp. 779–787 (2001)
41. Potapov, S., Maurel, B., Combescure, A., Fabis, J.: Modeling accidental-type fluid–structure interaction problems with the SPH method. Comput. Struct. **87**, 721–734 (2009)
42. Altomare, C., Crespo, A.J.C., Rogers, B.D., Dominguez, J.M., Gironella, X., Gómez-Gesteira, M.: Numerical modelling of armour block sea breakwater with smoothed particle hydrodynamics. Comput. Struct. **130**, 34–45 (2014)
43. Ferrari, A., Dumbser, M., Toro, E.F., Armanini, A.: A new 3D parallel SPH scheme for free surface flows. Comput. Fluids **38**(6), 1203–1217 (2009)
44. Shao, J.R., Li, H.Q., Liu, G.R., Liu, M.B.: An improved SPH method for modeling liquid sloshing dynamics. Comput. Struct. **100**, 18–26 (2012)
45. Viccione, G., Bovolin, V., Pugliese Carratelli, E.: Defining and optimising algorithms for neighbouring particle identification in SPH fluid simulations. Int. J. Numer. Methods Fluid **58**, 625–638 (2008)
46. Bovolin, V., Pugliese Carratelli, E.: , Viccione, G.: A numerical study of liquid impact on inclined surfaces. In: A. Bulucea, G. Viccione, C. Guarnaccia (eds.), Advances in Environmental and Geological Science and Engineering, Proceedings of

the 8th WSEAS International Conference on Environmental and Geological Science and Engineering (EG '15), vol. 38, pp. 218–223. Salerno, Italy, (2015)
47. Viccione, G., Bovolin, V., Pugliese Carratelli, E.: Simulating fluid-structure interaction with SPH. In: T. E. Simos (ed.), International Conference of Numerical Analysis and Applied Mathematics, Kos, Greece, 1479(209), pp. 209–212 (2012)
48. Viccione, G., Bovolin, V.: Simulating Triggering and Evolution of Debris-Flows with Smoothed Particle Hydrodynamics (SPH). Italian J. Eng. Geo. Environ. 523–532 (2011)
49. Viccione, G., Bovolin, V., Pugliese Carratelli, E.: Influence of the compressibility in Fluid–Structure interaction Using Weakly Compressible SPH. In: 4rd ERCOFTAC SPHERIC workshop on SPH applications. Nantes, France, pp. 407–412 (2009)
50. Batchelor, G.K.: An Introduction to Fluid Dynamics. Cambridge University Press, Cambridge (2000)
51. Monaghan, J.J., Gingold, R.A.: Shock simulation by the particle method SPH. J. Comput. Phys. **52**, 374–389 (1983)
52. Cleary, P.W.: Modelling confined multi-material heat and mass flows using SPH. Appl. Math. Model. **22**, 981–993 (1998)
53. De Padova, D., Darlymple, R.A., Mossa, M.: Analysis of the artificial viscosity in the smoothed particle hydrodynamics modelling of regular waves. J. Hydraul. Res. **52**(6), 13 (2014)
54. Molteni, D., Colagrossi, A.: A simple procedure to improve the pressure evaluation in hydrodynamic context using the SPH. Comput. Phys. Commun. **180**(6), 861–872 (2009)
55. Lee, E.S., Violeau, D., Issa, R., Ploix, S.: Application of weakly compressible and truly incompressible SPH to 3-D water collapse in waterworks. J. Hydraul. Res. **48**(Extra Issue), 50–60 (2010)
56. Das, R., Cleary, P.W.: Uniaxial compression test and stress wave propagation modelling using SPH. In: Fifth International Conference on Computational Fluid Dynamics in the Process Industries, Melbourne, Australia, p. 7 (2006)
57. Lennard-Jones, J.E.: Cohesion. Proc. Phys. Soc. **43**, 461–482 (1931)
58. Monaghan, J.J.: Simulating free surface flows with SPH. J. Comput. Phys. **110**, 399–406 (1994)
59. Viccione G., Bovolin V., Pugliese Carratelli, E.: Using SPH to compute slamming loads on vertical structures. In: 2nd International Conference on Violent Flows, pp. 261–266 (2012)
60. Flow Sciences Inc. Flow-3D User Manual, release 9.4, Santa Fe, NM, USA (2009)
61. Cavallaro, L., Dentale, F., Donnarumma, G., Foti, E., Musumeci, R.E., Pugliese Carratelli, E.: Rubble mound reakwater overtopping: estimation of the reliability of a 3D numerical simulation, In: ICCE 2012, International Conference on Coastal Engineering, Santander, Spain (2012)
62. Vanneste, D., Suzuki, T., Altomare, C.: Comparison of numerical models for wave overtopping and impact on storm return walls. In: ICCE 2014, International Conference on Coastal Engineering, Seoul, Korea (2014)
63. Rienstra, S.W., Hirschberg, a.: An Introduction to Acoustics. Eindhoven University of Technology, Eindhoven (2015)
64. Cooker, M.J., Peregrine, D.H.: Computations of violent motion due to waves breaking against a wall. In: Proceedings of 22nd International Conference Coastal Engineering Delft, Holland, pp. 164–176 (1990)
65. Bredmose, H., Hunt-Raby, A., Jayaratne, R., Bullock, G.N.: The ideal flip-through impact: experimental and numerical investigation. J. Eng. Math. **67**(1-2), 115–136 (2010)
66. Armanini, A., Larcher M., Odorizzi M.: Dynamic impact of a debris flow front against a vertical wall. In: Proceedings of the 5th International Conference on Debris-Flow Hazards Mitigation: Mechanics, Prediction and Assessment, Padua, Italy, pp. 1041–1049